ENERGY DEPENDENCE OF INCLUSIVE PHOTOPRODUCTION FOR DIFFERENT P_t AND ELECTRO-PRODUCTION OF VECTOR MESONS

J. GAYLER

DESY, Notkestr. 85, D-22603 Hamburg, Germany

Data are presented on the energy dependence of different reactions measured at HERA by the H1 and ZEUS collaborations. The energy dependence of inclusive photoproduction as function of the maximum p_t of the observed final state particles is related to the increase of the structure function F_2 versus small x for different Q^2. New results on the elastic production of vector mesons in γp and deep inelastic ep scattering are presented. The energy dependence and angular distributions are discussed. A significant enhancement is reported in the 4 pion mass spectrum in the reaction $ep \rightarrow e\pi^+\pi^-\pi^+\pi^- p$.

1 Introduction

At the collider HERA e^+p scattering is explored at the total e^+p invariant energy $\sqrt{s}$ in a wide range of squared momentum transfers Q^2 from the regime of quasi real photoproduction ($Q^2 \approx 0$) to deep inelastic scattering (DIS) at large space-like momentum transfer ($Q^2 > 0$), both with observation of the hadronic final state. The measurements at HERA therefore shed new light on the transition from hard scattering, where perturbative QCD is applicable, to the regime of soft hadronic interactions, where models of Reggeon-exchange and Vector Dominance are used to predict relations among different reactions.

The cross sections in these different regimes have characteristic energy dependences. Recently the H1 collaboration has phenomenologically parameterized the energy dependence of the structure function F_2 at fixed Q^2 as $\sim x^{-\lambda}$, where x is the Bjorken scaling variable which is related to the invariant mass W of the virtual-photon ($\gamma^* p$) system by $W^2 = Q^2(1/x - 1)$. The parameter $\lambda(Q^2)$ was shown [1] to rise in the range $1 < Q^2 < 1000$ GeV^2 from about 0.2 to 0.4. If the structure function is related to a virtual photon total absorption cross section by

$$\sigma^{tot}_{\gamma^* p}(W, Q^2) = \frac{4\pi^2\alpha}{Q^2} F_2(W, Q^2) \quad ,$$

the dependence $F_2 \sim x^{-\lambda}$ corresponds at small x to an energy dependence of the total cross section at fixed Q^2 like

$$\sigma^{tot}_{\gamma^* p} \sim (W^2)^{\lambda} \quad .$$

Whereas the increase of the steepness with Q^2 of the x-dependence (or W^2-dependence) of the structure function can be interpreted in perturbative QCD using the DGLAP evolution equations, this parameter λ, which governs the energy dependence, is related in Regge theory to the Regge trajectory intercept at $t = 0$

$$\alpha(t) = 1 + \lambda + \alpha' t \quad ,$$

with t the momentum transfer squared to the initial state proton.

The energy dependence of the total photoproduction cross section as well as that of elastic ρ^0 or ω meson production are well described by $\lambda \approx 0.08$, a value known from soft hadronic interactions [2] as the intercept of the "soft pomeron". In the spirit of Capella at al. [3] (CKMT model) the steeper energy dependence of hard processes can be interpreted as being due to larger effective trajectory intercepts at large values of Q^2, p_t or the produced masses, as these cross sections are small and no unitarity corrections to one pomeron exchange are needed here.

The results from the ep-collider HERA help to understand the relationship between the concepts of Reggeon exchange and perturbative QCD.

2 Inclusive Photoproduction for different observed maximum p_t

Whereas in DIS the hardness of the interaction can be characterized by the momentum transfer squared Q^2, it is the large p_t of final state hadrons which indicates a hard scattering process in photoproduction ($Q^2 \approx 0$).

For the interaction with the proton a high value of Q^2 may indeed play a similar role as production of high p_t particles in the photon fragmentation region as sketched in figure 1.

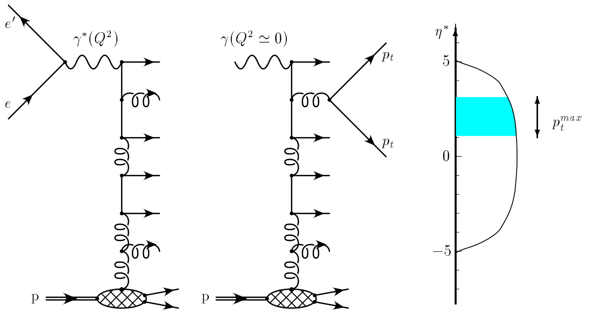

Figure 1: Diagrams for a DIS and for a photoproduction event with high p_t particles (jets) in the final state. The sketch on the right-hand side indicates an inclusive charged particle rapidity distribution in the γp center of mass system and the range used for the search of high p_t tracks.

Photoproduction events were selected [4] by detection of the scattered e^+ in the "electron tagger" of the H1 luminosity system [5] in the scaled energy range $0.25 < y = 1 - E_{e'}/E_e < 0.70$, where E_e and $E_{e'}$ are the initial and scattered positron energies respectively. This corresponds to the range $150 < W_{\gamma p} < 250$ GeV, in which the W dependence is measured for different observed maximum transverse momenta, p_t^{max}, of charged particle tracks in the pseudo-rapidity range $1.1 < \eta^* < 3.1$ (fig. 1). Here $\eta^* = -\ln(\tan(\theta^*/2))$ is the pseudo-rapidity in the γp center of mass system, where the polar angle θ^* is measured with respect to the γ direction.

Fig. 2 shows that the steepness of the energy dependence of the observed ratio $\tilde{R}$ of events in a given range of maximum p_t to all tagged events increases with p_t.

The final fully corrected slope parameters λ are presented in fig. 3a. A linear fit $\lambda = C \cdot \ln(4p_t^2) + \lambda_0$ (solid line in fig. 3a) gives $C = 0.112 \pm 0.007$ and $\lambda_0 = 0.031 \pm 0.014$. Note that other multiplicative factors to p_t^2 will not change the value C of the 'scale' dependence.

The comparison with the QCD based event generator PYTHIA [6] shows good agreement (fig. 3a), and further, that phase space effects play only a minor role. In PYTHIA most of the effect is given by the leading order QCD matrix element.

We observe a striking qualitative similarity with the results obtained in DIS [1] (fig. 3b): the harder the scale ($4p_t^2$ and Q^2 respectively), the steeper the rise with energy of the real or virtual photoproduction cross section respectively.

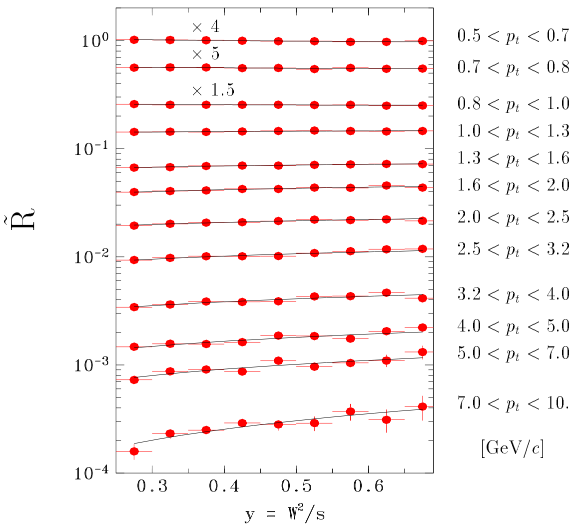

Figure 2: Energy dependence of the ratio $\tilde{R}$ in different bins of the maximum p_t observed in the pseudo-rapidity range $1.1 < \eta^* < 3.1$. The curves represent fits $\tilde{R} = W^{2 \cdot \tilde{\lambda}}$.

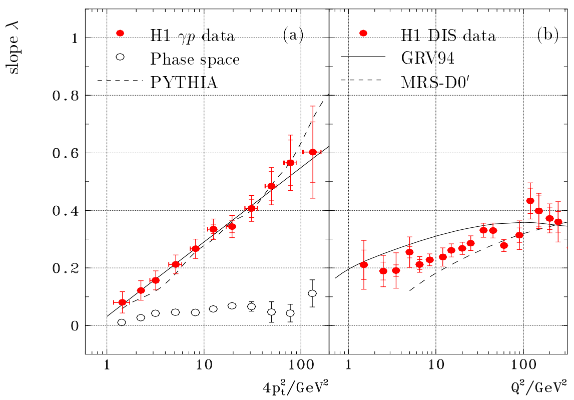

Figure 3: a) photoproduction: slope λ of the W^2 dependence as function of the scale $4p_t^2$ given by the selected maximum p_t particle. The full line represents a linear fit $\lambda = C \cdot \ln(4p_t^2) + \lambda_0$ with parameters given in the text. b) DIS: slope λ of the proton structure function F_2 as function of Q^2 [1] in comparison with different parameterizations of parton densities.

3 Elastic Vector Meson Production

New data on vector meson production in photoproduction and DIS have been submitted by the H1 and ZEUS collaborations to this conference. New results from ZEUS not referring to J/ψ-photoproduction are discussed in other talks [7,8]. For further new results from H1 on vector meson production, not touched in this talk, see refs. [9].

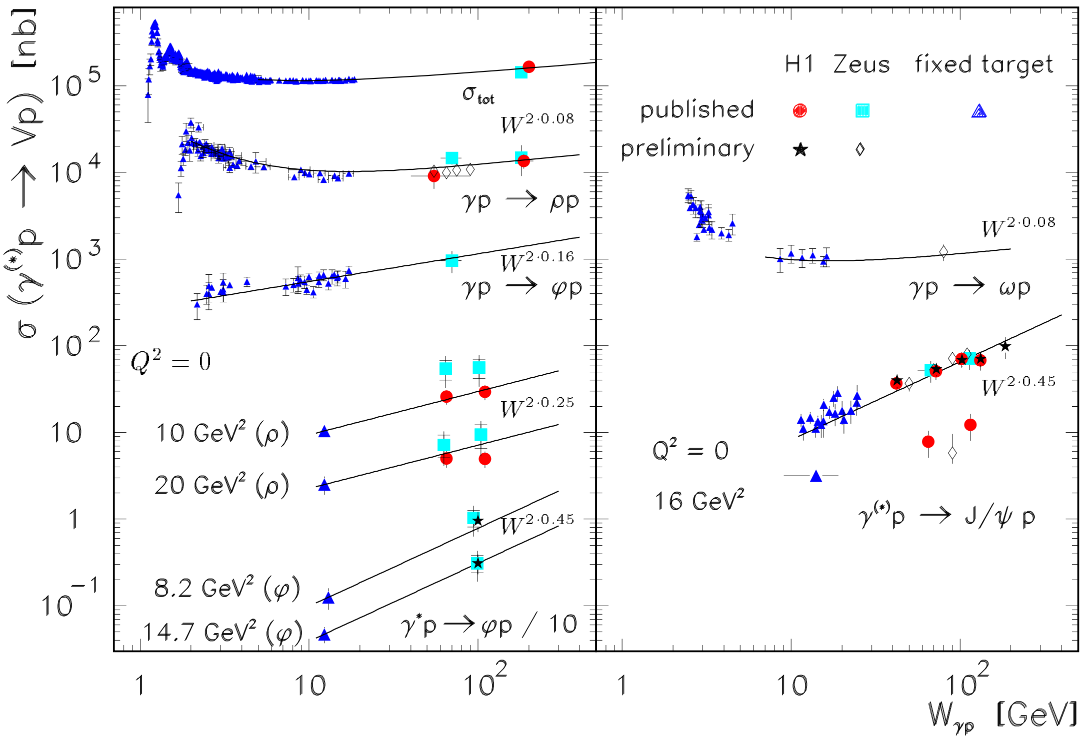

Figure 4: Elastic production of vector mesons as function of $W_{\gamma p}$ at $Q^2 \approx 0$ and $Q^2 > 8$ GeV^2. The curves for the total cross section [10] and ρ^0 [11], ω [11] and ϕ [10] photoproduction are based on pomeron exchange. Additional linear dependences are shown to guide the eye. The power of the W dependence is indicated.

3.1 Photoproduction of ρ^0, ω, ϕ and J/ψ Mesons

In photoproduction the energy dependencies of the cross sections for the production of the light vector mesons ρ^0 and ω is rather flat as for the total γp cross section (fig. 4). These data are well compatible with an energy dependence $\sim (W^2)^\lambda$ with $\lambda = 0.08$ as expected from soft hadronic interactions [2].

For the heavy vector meson J/ψ a steeper energy dependences is observed, qualitatively similar to the results of the previous section, where such behaviour was observed by increase of the involved scales p_t^2 or Q^2 instead of the mass.

The cross section for elastic photoproduction of J/ψ mesons is expected to be proportional to the square of the gluon density of the proton due to gluon ladder graphs. The data in fig. 5 are indeed well described by the model of Ryskin [12] using the parton densities of MRSA' [13]. However uncertainties of the normalization of the calculations still prevent a direct determination of the gluon density by this reaction.

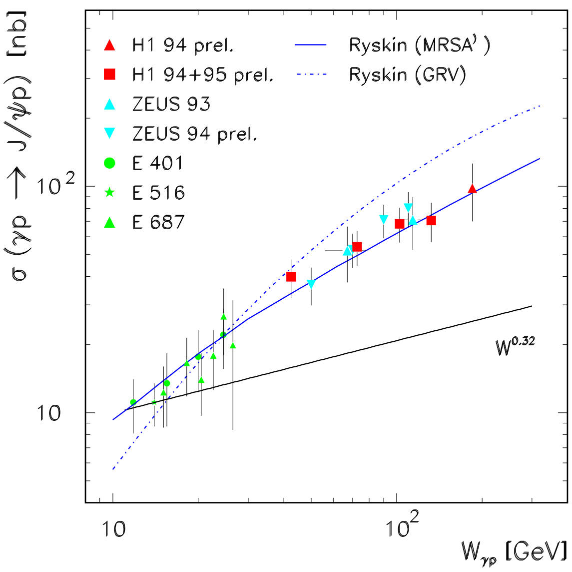

Figure 5: Energy dependence of the cross section for elastic J/ψ photoproduction in comparison to the model of Ryskin [12] using different parton densities. The dependence $\sim W^{2\cdot 0.16}$ expected [10] from soft hadronic interactions is shown for comparison.

Both collaborations, H1 [14] and ZEUS [15] agree on the slope b of the t-distribution $\exp(-bt)$ of J/ψ production with $b = 4.1 \pm 0.2 \pm 0.2$ GeV^{-2} and $b = 4.0 \pm 0.4^{+0.6}_{-0.7}$ GeV^{-2} respectively. There is some indication (1.5σ level) of an increase of this slope with energy ("shrinkage" expected in Regge theory) as shown by H1 by splitting the data in ranges $W < 90$ and $W > 90$ GeV [14]. Consideration of fixed target experiments does not allow a clear conclusion on shrinkage at the present level of experimental precision.

The decay angular distribution of J/ψ mesons shows [15] that the J/ψ are predominantly transversely polarized (like the virtual photon at $Q^2 \approx 0$) consistent with s-channel helicity conservation (SCHC).

3.2 Elastic Production of Vector Mesons in DIS

The decay angular distributions of ρ^0, ω, ϕ mesons change drastically going from photoproduction to the DIS regime ($Q^2 \gtrsim 5$ GeV^2). The probability to observe a longitudinally polarized vector meson, i.e. the spin-density matrix element r^{04}_{00}, changes from $Q^2 = 0$ to $Q^2 > 8$ GeV^2 as measured by H1 [16,17] (as also reported by ZEUS [18]) for ρ^0 production, e.g., from $r^{04}_{00} = -0.11 \pm 0.11 \pm 0.04$ to $r^{04}_{00} = 0.73 \pm 0.05 \pm 0.02$ indicating a ratio of the longitudinal to transverse cross section $R = \sigma_L/\sigma_T \approx 2.7$ assuming SCHC. Similarly H1 measured for ϕ production $r^{04}_{00} = 0.77 \pm 0.11 \pm 0.02$ corresponding to $R \approx 3.3$ assuming SCHC [19].

For $Q^2 > 10$ GeV^2 a strong rise of the cross section with W is observed also for the light ρ^0 meson besides ϕ and J/ψ (fig. 4). Whereas at $Q^2 = 0$ the ρ^0 cross section is more than a factor 100 above the J/ψ cross section and about a factor 10 above the ϕ cross section, the SU4 symmetry [20] ($\sigma(\phi)/\sigma(\rho^0) = 2/9$, $\sigma(J/\psi)/\sigma(\rho^0) = 8/9$) is roughly fulfilled at $Q^2 \gtrsim 10$ GeV^2. But will this symmetry survive future data at even larger Q^2?

3.3 Enhancement in the $\pi^+\pi^-\pi^+\pi^-$ Mass Spectrum

H1 observes a strong enhancement in the 4 pion mass spectrum around 1.6 GeV, predominantly in the elastic reaction $ep \to e\pi^+\pi^-\pi^+\pi^- p$ (fig. 6) [21]. Only the 4 pions are detected from the hadronic final state, but the mass of the unobserved hadronic system is $\lesssim 1.6$ GeV. The 4 pion state in the resonance peak in figure 6 has a strong ρ^0 contribution in the $\pi^+\pi^-$ subsystems. A fit to the 4 pion mass distribution assuming a single ρ' state yields mass $m_{\rho'} = 1.57 \pm 0.02 \pm 0.01$ and width $\Gamma_{\rho'} = 0.18 \pm 0.06 \pm 0.07$. If fitted by a superposition of $\rho(1450)$ and $\rho(1700)$ states, the two resonances contribute with about equal strength and opposite phases. With the present limited statistics no definite conclusions on the composition of the state can be drawn. The size of the signal is however remarkable. As shown in figure 7 the ratio $\sigma(\rho')/\sigma(\rho^0)$ increases from $Q^2 \approx 0$ to $Q^2 \approx 11$ GeV^2 from about 0.1 to about 0.3. This rise may be explained [22] in the framework of QCD by cancellations due to nodes in the wave function of the produced $q\bar{q}$-system, which are no longer felt if it is probed by a small size γ^* at high Q^2.

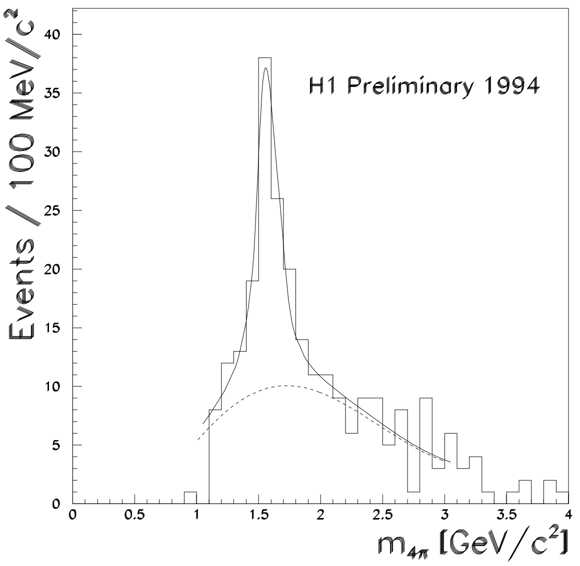

Figure 6: Distribution of $m_{4\pi}$ of the reaction $ep \to e\pi^+\pi^-\pi^+\pi^- p$. The solid line is the result of a fit to a single resonance with free mass and width over a polynomial background (broken line).

4 Summary

The energy dependence of various cross sections was shown to get steeper once any of the scales Q^2, p_t^2 or the involved vector meson masses gets large. This was demonstrated for inclusive photoproduction as function of the maximum p_t observed in the final state in the photon fragmentation region. This rise can qualitatively be compared to the rise

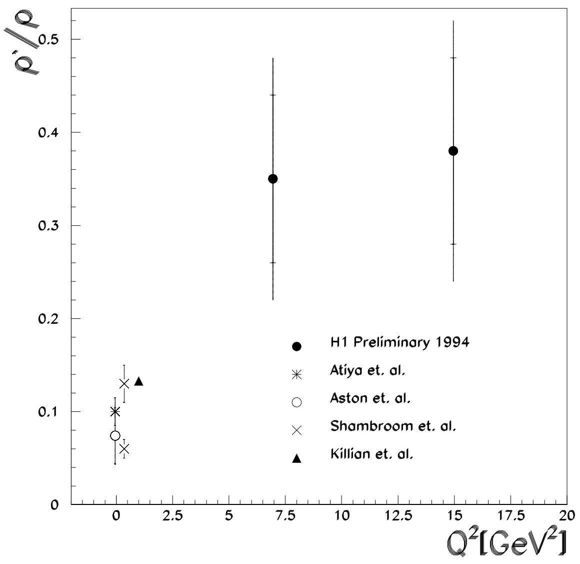

Figure 7: Ratio $\sigma(\rho')/\sigma(\rho^0)$ as function of Q^2 in comparison with fixed target experiments[23].

of the inclusive structure function F_2 in DIS with decreasing x. In elastic vector meson production the $\gamma p \to J/\psi p$ cross section increases rapidly with energy at $Q^2 = 0$. This can be explained by the strong rise observed for the proton gluon density at small x. A corresponding rise with energy is observed for light vector mesons also at large momentum transfers $Q^2 \gtrsim 5$ GeV^2.

The decay angular distributions of ρ^0, ϕ and J/ψ mesons in elastic photoproduction show that the mesons are transversely polarized consistent with SCHC. In electroproduction at $Q^2 \gtrsim 6$ GeV^2 the ρ^0 and ϕ mesons are predominantly longitudinally polarized, implying $R = \sigma_L/\sigma_T \approx 3$ assuming SCHC.

Finally, a ρ' enhancement in the 4π mass spectrum was observed in the reaction $ep \to e\pi^+\pi^-\pi^+\pi^- p$. The observed ratio $\sigma(\rho')/\sigma(\rho^0)$ at $< Q^2 > \approx 11$GeV^2 is about 3 times larger than measured at fixed target experiments at low Q^2 and low W.

Acknowledgments

I am grateful to R. Eichler, S. Levonian and Arndt Meyer for help in the preparation of this talk and to J. Dainton for a careful reading of the manuscript.

References

1. H1 Collab., S. Aid *et al*, *Nucl. Phys.* B **470**, 3 (1996).
2. H. Cheng, J.K. Walker, T.T. Wu, *Phys. Lett.* B **44**, 97 (1973),
   A. Donnachie and P. Landshoff, *Nucl. Phys.* B **244**, 322 (1984), ibid. **267**,690 (1985).
3. A. Capella, A. Kaidalov, C. Merino and J. Tran Thanh Van, *Phys. Lett.* B **337**, 358 (1994).
4. H1 Collab., contributed paper pa02-79.
5. H1 Collab., I. Ahmed *et al*, *Z. Phys.* C **66**, 529 (1995).
6. T.Sjőstrand, *CERN-TH*-6488 (1992), *Comp. Phys. Commun.* **82**, 74 (1994).
7. J. Buhlman, these proceedings.
8. O. Lukina, these proceedings.
9. H1 Collab., contributed papers pa02-65, pa02-86.
10. A. Donnachie and P. Landshoff, *Phys. Lett.* B **296**, 227 (1992), ibid. **348**,213 (1995).
11. G.A. Schuler, T. Sjőstrand, *Nucl. Phys.* B **407**, 539 (1993).
12. M.G. Ryskin,*Z. Phys.* C **57**, 89 (1993), M.G. Ryskin et al.,DTP-95-96, RAL-TR-95-065.
13. A.D. Martin, W.J. Stirling and R.G. Roberts, *Phys. Lett.* B **354**, 155 (1995).
14. H1 Collab., contributed paper pa02-085.
15. ZEUS Collab., contributed paper pa02-47.
16. H1 Collab., S. Aid *et al*, *Nucl. Phys.* B **463**, 3 (1996).
17. H1 Collab., S. Aid *et al*, *Nucl. Phys.* B **468**, 3 (1996), contributed paper pa02-66.
18. ZEUS Collab., M. Derrick *et al*, *Z. Phys.* C **69**, 39 (1995), *Phys. Lett.* B **356**, 601 (1995).
19. H1 Collab., contributed paper pa02-64.
20. E.M. Levin and L.L. Frankfurt, *JETP Lett.* **2**, 65 (1965), H.J. Lipkin and F. Scheck, *Phys. Rev. Lett.* **16**, 71 (1966), H. Joos, *Acta Physica Austriaca, Suppl.***IV***,320 (1967).*
21. H1 Collab., contributed paper pa01-88.
22. B.Z. Kopeliovich *et al*, *Phys. Lett.* B **309**, 179 (1993).
23. M.S. Atiya et al.,*Phys. Rev. Lett.* **43**, 1691 (1979), D. Aston et al.,*Nucl. Phys.* B **189**, 15 (1981), W.D. Shambroom et al.,*Phys. Rev.* D **26**, 1 (1982), T.J. Killian et al.,*Phys. Rev.* D **21**, 3005 (1980).